
This is an electronic reprint of the original article.
This reprint may differ from the original in pagination and typographic detail.

Savolainen, Henri; Backholm, Matilda; Ikkala, Olli; Zhang, Hang
Light-triggered Time-Programmed Self-adhesion in Low-Hysteresis Hydrogels

Published in:
ACS Applied Polymer Materials

DOI:
[10.1021/acsapm.3c02117](https://doi.org/10.1021/acsapm.3c02117)

Published: 12/01/2024

Document Version
Publisher's PDF, also known as Version of record

Published under the following license:
CC BY

Please cite the original version:
Savolainen, H., Backholm, M., Ikkala, O., & Zhang, H. (2024). Light-triggered Time-Programmed Self-adhesion in Low-Hysteresis Hydrogels. *ACS Applied Polymer Materials*, 6(1), 433-440.
<https://doi.org/10.1021/acsapm.3c02117>

This material is protected by copyright and other intellectual property rights, and duplication or sale of all or part of any of the repository collections is not permitted, except that material may be duplicated by you for your research use or educational purposes in electronic or print form. You must obtain permission for any other use. Electronic or print copies may not be offered, whether for sale or otherwise to anyone who is not an authorised user.

Light-triggered Time-Programmed Self-adhesion in Low-Hysteresis Hydrogels

Henri Savolainen, Matilda Backholm, Olli Ikkala,* and Hang Zhang*

Cite This: *ACS Appl. Polym. Mater.* 2024, 6, 433–440

Read Online

ACCESS |

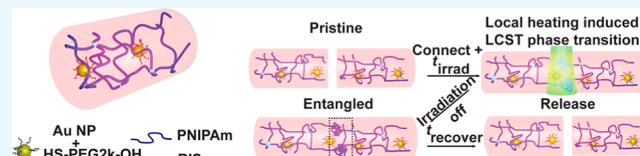
Metrics & More

Article Recommendations

Supporting Information

ABSTRACT: Self-healing of hydrogels has attracted intensive research based on dynamically exchangeable bonds. However, this typically leads to decreased elasticity and increased energy dissipation during mechanical deformations, which is not desirable in, for example, soft robotic applications. Thus, there exists an unmet demand for low hysteresis, that is, resilient, materials to quickly recover the mechanical properties after damage. Here, we show low-hysteresis chemically cross-linked hydrogels with on-demand local light-triggered fast self-adhesion, with time-dependent adhesion strength controlled by the duration of irradiation. Low mechanical hysteresis is achieved by swelling of the loosely cross-linked poly(*N*-isopropylacrylamide) network. Rapid self-adhesion is followed by localized photothermal heating of embedded gold nanoparticles, causing collapse and promoting local entanglements of the thermoresponsive poly(*N*-isopropylacrylamide) chains. This provides 95.7% initial recovery of the original mechanical properties, while the interface undergoes gradual rehydration and disentanglement depending on the irradiation details, leading to a decrease of the adhesive strength to zero within 7 h. The concept can be combined with conventional slow self-healing that is allowed by additional clay nanoplatelets for long-standing healing. The application potential is demonstrated by oscillations, time-programmed release of the adhered object, and on-demand assembly of designed hydrogel shapes. The proposed mechanism with facile, efficient, and light-controlled temporal profiles that are time-programmed can be applied to soft robotics, biomedical applications, and flexible electronics.

KEYWORDS: self-adhesion, resilience, hydrogels, light, self-healing



1. INTRODUCTION

In the past decade, self-healing hydrogels have attracted significant research interest, since they can greatly enhance the durability and safety of soft devices, offering enormous application potential in soft robotics, tissue engineering, and drug release.^{1,2} The self-healing mechanisms typically involve dynamically exchangeable covalent bonds^{3–6} or physical interactions, such as hydrogen bonding,⁷ electrostatic interactions,⁸ hydrophobic interactions,⁹ and host–guest interactions.¹⁰ However, the mechanisms providing self-healing properties such as using ionic bonds often lead to energy dissipation during mechanical deformations, that is, leading to hysteresis loop during cyclic tensile tests.^{8,11} Low hysteresis, that is, resilience in cyclic mechanical tensile tests has recently emerged as an attractive property in hydrogels, which could provide low energy loss and high reversibility during deformations, highly desirable for, e.g., soft robotic applications.^{12,13} Despite the promising potential of combining low hysteresis with self-healing in soft materials, only few examples of self-healing polymeric materials with low mechanical hysteresis exist so far,^{14,15} due to the intrinsic limitations of self-healing materials to date.

On the other hand, various mechanisms for hydrogel adhesion have been developed, which rely on the synergy of chemistry, topology, and mechanics.¹⁶ Recent studies have

focused on stimuli-triggered hydrogel adhesion mechanisms, for example, based on pH change,¹⁷ electrical stimulus,¹⁸ temperature,¹⁹ and UV light.²⁰ Photodetachable adhesion of hydrogels has been achieved by utilizing light-sensitive stitching polymer networks, which undergo sol–gel transition upon UV irradiation.²⁰ Recently, self-adhesion in hydrogels has been highly sought after in tissue engineering^{21,22} and bioelectronics.²³ In this study, we will explore light-triggered transient self-adhesion in resilient hydrogels with low hysteresis, where the recovery efficiencies are comparable to self-healing hydrogels. We exploit strong self-adhesion based on polymer entanglements across the interfaces, induced by local photothermal heating using embedded gold nanoparticles (AuNPs) and subsequent thermoreversible phase transition (lower critical solution temperature, LCST) of the poly(*N*-isopropylacrylamide) (PNIPAm) gel matrix. We examine the hypothesis that phase-transition-induced entanglement can be used for self-adhesion, where PNIPAM is suitable for the

Received: September 7, 2023

Revised: November 17, 2023

Accepted: November 17, 2023

Published: December 1, 2023



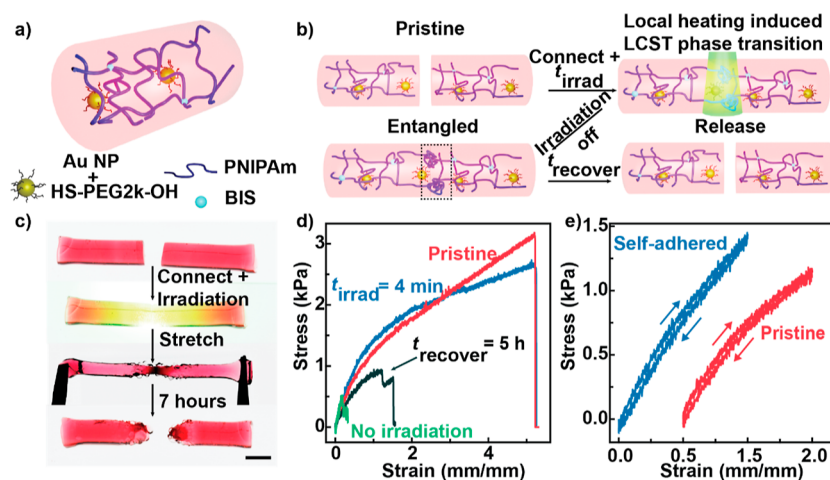


Figure 1. Light-triggered self-adhesion based on polymer entanglement at the interface. (a) Structure of the PNIPAm hydrogel. (b) Schematic illustration of the polymer entanglement–disentanglement mechanism, wherein the dotted region highlights the entanglement of the chains. (c) Photographs of the hydrogel during the self-adhesion process. Scale bar represents 6 mm. (d) Comparison of the pristine sample, sample adhered without irradiation, and self-adhered samples right after or 5 h after irradiation. (e) Comparison of pristine and self-adhered samples in cyclic tensile testing. The strain of the pristine sample is shifted by 0.5 for clarity. Tensile tests have been repeated at least 3 times.

transition and gold nanoparticles for photothermal heating. Unlike classic self-healing with dynamically reconstituting dynamic bonds, such an approach could allow reduced hysteresis in cyclic loading, that is, reduced energy dissipation and thus promoted resilience. The duration of irradiation and its effect on the recovery efficiency of the resilient gel are studied. The resilience of the hydrogel and the time scale of self-adhesion are investigated by various control experiments. The mechanism was further explored by time-development studies of adhesion and simulation of temperature distribution during the photothermal heating process. Notably, the self-adhesion mechanism can be synergistically coupled to more conventional self-healing mechanisms. This provides additional temporal control over the interfacial strength, in contrast to time-dependent self-healing, which is useful for constructing complex shapes using light-driven adhesions.

2. RESULTS AND DISCUSSION

2.1. Resilient and Self-Adhesive AuNPs/PNIPAm Hydrogels. Though nanocomposite hydrogels based on gold nanoparticles and PNIPAm have long been explored for their photothermally triggered volumetric changes and actuation, e.g., for soft robotics,^{24,25} their self-adhesive and resilient properties have not been explored. The dynamic bonds employed for self-healing are expected to decrease the resilience of the material, as also shown in cyclic compression tests in a Au–thiolate coordination system.²⁶ Here, we demonstrate that high resilience can be achieved by extensive swelling of a loosely cross-linked PNIPAm network, while fast localized photothermal heating at the contact surface can lead to on-demand strong temporary self-adhesion, as shown in Figure 1. The hydrogel consists of PEGylated 14.5 ± 0.9 nm gold nanoparticles (Figure S1) embedded in a PNIPAm network cross-linked by *N,N'*-methylenebis(acrylamide) (BIS), as shown in Figure 1a. To synthesize the hydrogel, an aqueous monomer solution containing 13.8 wt % NIPAm, 0.86 wt % AuNPs, and 0.046 mol % BIS relative to NIPAm was polymerized by the addition of the initiator ammonium persulfate (APS) and accelerator *N,N,N',N'*-tetramethylethylenediamine (TEMED). After polymerization, the gel samples were

removed from the glass tube and left to swell in deionized water overnight, where the diameter of the samples increased from 4.1 to 6.0 mm; the swelling ratio over time is listed in Figure S2a. The obtained gels had a characteristic transparent red appearance due to the presence of AuNPs. The LCST of the hydrogel was determined to be 34 °C by transmittance measurements (Figure S2b). The self-adhesion of the hydrogel is schematically shown in Figure 1b. The strength of the self-adhesion was characterized by the adhesion strength between two end-to-end attached hydrogels. The swollen hydrogel has low self-adhesion at room temperature due to lack of strong interactions between the PNIPAm chains, as shown in Figure 1d. Upon irradiation with an LED at 525 nm (8.49 W/cm^2), close to the absorption maximum of the AuNPs (Figure S1c), the interfacial strength dramatically improves due to the light-induced local heating and subsequent collapse and phase transition of PNIPAm. This promotes entanglements of PNIPAm chains due to hydrophobic interactions, as the PNIPAm chains become hydrophobic above the LCST.²⁷ The entanglement enables an interfacial strength comparable to that of the pristine hydrogel right after irradiation at room temperature (Figure 1c,d), where 4 min irradiation leads to the recovery of an ultimate tensile stress of $105 \pm 24.6\%$ and a strain of $95.7 \pm 25.5\%$. Figure 1c shows that the local heating also caused dehydration of the hydrogel, where the hydrogel at the irradiated region shrunk by 42% in diameter. Once the irradiation is switched off, the hydrogel is cooled down to room temperature, and the PNIPAm becomes hydrophilic again, while the entanglement remains temporarily. Thus, the strength of adhesion is time-dependent and decreases gradually as the dehydrated region becomes rehydrated by the water diffusion from the bulk of the hydrogel. After 7 h at room temperature, the sample splits as the adhesion loses its strength (Figure 1c).

In addition to the light-triggered self-adhesion, the swollen AuNPs/PNIPAm hydrogel is also resilient, which is a highly desirable property for soft robotic applications, where precise control over the deformation and reversibility depends on the resilience of the material.²⁸ As shown in Figure 1e, the cyclic tensile tests of both the pristine and self-adhered hydrogels

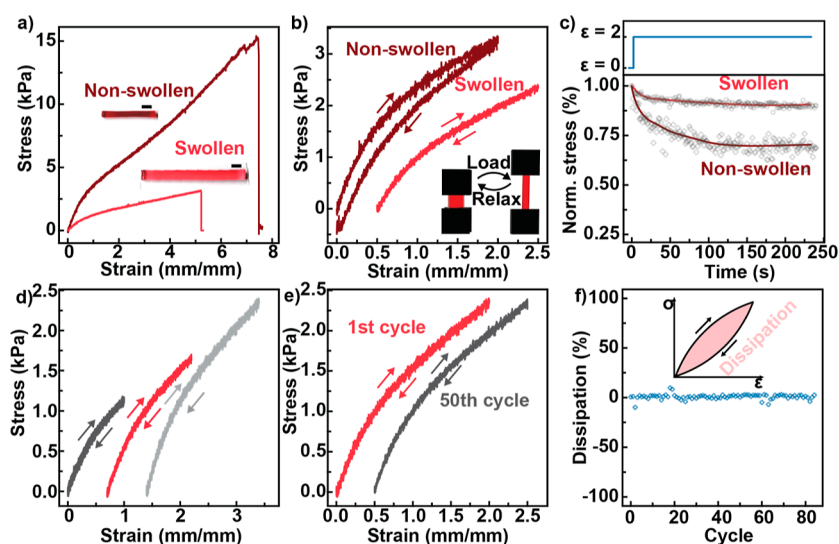


Figure 2. Investigation of the resilience in the AuNPs/PNIPAm hydrogel. (a) Change in mechanical properties in tensile testing after swelling. Scale bar: 6 mm. (b) Comparison of hysteresis in swollen and nonswollen hydrogels. The swollen sample is shifted by 0.5 for clarity. Each measurement represents the first cycle. (c) Step strain relaxation tests of swollen and nonswollen hydrogels. Solid lines serve as a guide for the eye. (d) Resilience at different tensile strains of the swollen hydrogel. Data are shifted by a strain of 0.65 for second measurement and 1.3 for third measurement for clarity. Each measurement represents the first cycle. (e) Resilience preserved after 50 cycles of testing. Data are shifted by a strain of 0.5. (f) Dissipation of energy in 80 cycles and an illustration of dissipation. Tensile tests have been repeated at least 3 times.

show only a small hysteresis loop. Recent reports have demonstrated several mechanisms to achieve resilience, such as strain-induced crystallization in a slide ring hydrogel,²⁹ nanoparticle-reinforcement in a nanocomposite hydrogel,³⁰ and gelatin-based biogels.³¹ In the current AuNPs/PNIPAm system, the resilience is a result of the low cross-linking degree and swelling, that is, extensive stretching of the network. Control experiments demonstrate that higher cross-linker concentrations leads to increasing hysteresis (Figure S3a), while the addition of AuNPs only leads to minor strengthening of the PNIPAm and did not alter the resilience of the system (Figure S3b). In addition, the resilience is not limited to the PNIPAm hydrogel, as hydrogels synthesized with acrylamide monomers also exhibit similar resilience (Figure S3c). Raising the PNIPAm content to 20 wt % and reducing the BIS concentration to 0.0001 mol % also led to similar results in terms of resilience (Figure S3d).

2.2. Resilience in AuNPs/PNIPAm Hydrogels. Figure 2 demonstrates different aspects related to the resilience of the present hydrogel. Figure 2a illustrates the stress–strain curves for AuNP/PNIPAm hydrogels in nonswollen and swollen states. As mentioned above, a low cross-linker concentration and a high swelling degree result in resilience and low hysteresis in the AuNPs/PNIPAm hydrogels, which align with previous reports on polyacrylamide hydrogels.^{13,30} During swelling, the network of the hydrogel significantly expands, thus reducing the polymer–polymer interactions.¹³ Therefore, the dissipative interactions decrease, and the hydrogel acts predominantly as an elastic spring.³² Swelling reduced the ultimate tensile strength of the sample from 11.9 ± 1.6 kPa at a strain of 8.3 ± 1.8 to 2.3 ± 0.7 kPa at a strain of 4.8 ± 1.5 due to the stretching of the chains (Figure 2a). The swollen PNIPAm samples have lower mechanical strength and maximum elongation, which have been commonly observed in other hydrogels.³³ Commonly, the strengthening mechanism of nanoparticles is caused by the interaction of the nanoparticles with the network via physical interactions as

hydrogen bonds.³⁴ In the case of gold nanoparticles, the surface does not employ any specific interactions with the polymer chain to have a noticeable increase in mechanical strength. Besides, the concentration of AuNPs in the hydrogel is 0.86 wt %, much lower than that of common nanocomposite hydrogels using a filler content of few wt %. Notably, swelling results in the reduction of the hysteresis during cyclic tensile testing, as shown in Figure 2b. Swelling is commonly attributed in many hydrogels to be the key factor for obtaining low hysteresis in cyclic tensile testing because water can act as a lubricant with its low viscosity and it reduces the polymer–polymer interactions.^{30,35} The effect of the swelling can be seen in Figure 2b,c. The dissipation of nonswollen samples is $17.3 \pm 5.7\%$ and swollen samples is $2.5 \pm 2.1\%$, as seen in Figure S4b. Figure 2d shows the high resilience of the hydrogel up to a strain of 2, above which some degree of hysteresis appears as a result of energy dissipation due to, e.g., rupture of bonds and irreversible disentanglement.¹³ Furthermore, resilience and low viscosity also contributed to low fatigue, as elastic deformation prevails. Even after 50 cycles up to a strain of 2, the tensile curve stays practically invariant with the same low hysteresis (Figure 2e). The resilience can be characterized by the dissipation of the elastic energy during the tensile test, using the area below the tensile curves during loading (often denoted as the modulus of toughness) and the corresponding unloading cycles, as shown in eq 1 and Figure 2f.

$$\text{Dissipation} = \frac{A_{\text{load}} - A_{\text{unload}}}{A_{\text{load}}} \times 100\% \quad (1)$$

where A_{load} is the area below the loading tensile curve (i.e., modulus of toughness) and A_{unload} is the area below the unloading tensile curve. The dissipation thus indicates the area between the two curves, where 0% indicates no dissipation in the elastic energy and 100% indicates full dissipation in the elastic energy. As shown in Figure 2f, the dissipation of the AuNPs/PNIPAm hydrogel is typically at $0.8 \pm 5.7\%$ during the 80 measured cycles, where the negative and deviating values

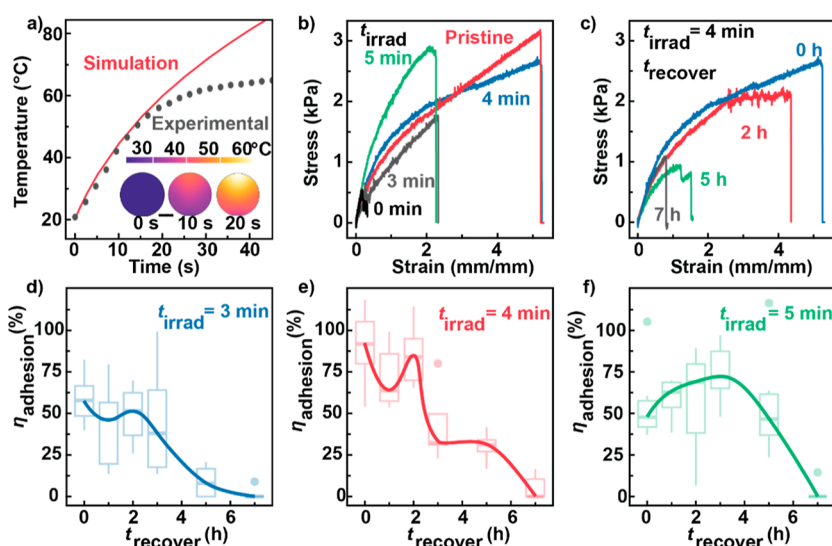


Figure 3. Light-triggered self-adhesion in the AuNPs/PNIPAm hydrogel. (a) Temperature evolution of the hydrogel upon irradiation starting at $t = 0$ s. Insets show the cross-sectional distribution of temperature from simulation. (b) Effect of irradiation duration on the optimal self-adhesive strength. (c) Tensile properties of an irradiated sample ($t_{\text{irrad}} = 4$ min) at different recovery times (t_{recover}). (d) Time evolution of the adhesion efficiency after 3 min of irradiation. (e) Time evolution of the adhesion efficiency after 4 min of irradiation. (f) Time evolution of the adhesion efficiency after 5 min of irradiation. Curves are given as an eye guide for the boxplots. Tensile tests have been repeated at least 5 times.

are a result of noise error in the measurement (the unloading curve is higher than the loading curve of cycles, see Figure S4a.)

2.3. Light-Triggered Self-Adhesion in AuNPs/PNIPAm Hydrogels. We next studied the influence of irradiation on the self-adhesion process in Figure 3. The temperature change of the hydrogel was measured by an IR camera and simulated using the finite-element method in COMSOL (Figure 3a). Upon irradiation, the maximum temperature measured from the side of the hydrogel shows a quick increase in the first 20 s, where it reaches the LCST at 8 s. This time interval can be accurately simulated, and the internal temperature distribution at the cross-section of the hydrogel from the simulation is shown in the insets in Figure 3a and Figure S5. Due to light absorption by the AuNPs, a gradient of temperature exists at the cross-section of the hydrogel. The temperature difference between the top surface (incidence of light) and the bottom surface reached around 24 °C at 20 s (Figure S5a). At $t = 20$ s, the temperature of the whole cross-section is above the LCST of the hydrogel at 34 °C. The simulation deviates substantially from the measured results after 20 s, which can be attributed to increased shrinking and dehydration of the hydrogel, evaporation of the exuded water, and scattering of light due to phase transition, which are not included in the simulation.

The influence of the irradiation time (t_{irrad}) on the self-adhesion strength is shown in Figure 3b. Here, we define the self-adhesion efficiency η_{adhesion} as the ratio between the tensile strain at failure of a self-adhered ($\epsilon_{\text{adhered}}$) sample and that of a pristine sample ($\epsilon_{\text{pristine}}$) in eq 2.

$$\eta_{\text{adhesion}} = \frac{\epsilon_{\text{adhered}}}{\epsilon_{\text{pristine}}} \times 100\% \quad (2)$$

A minimum t_{irrad} is required to maintain the adhesion after irradiation stops, as shown in Figure 3b. The stress-relaxation test of a sample irradiated for 1 min in Figure S6 shows the detachment of the sample right after the removal of light at a strain of 1. Optimum self-adhesion is achieved at $t_{\text{irrad}} = 4$ min, where the recovery of a tensile strain of $95.7 \pm 25.5\%$ can be

achieved compared to the pristine hydrogel. For irradiation at a shorter duration, e.g., 3 min, the phase transition is not sufficient to achieve strong entanglement at the interface, and the recovery efficiency is $58.9 \pm 14.7\%$. After 3 h, the adhesion efficiency is greater for 3 and 5 min of irradiation than for 4 min of irradiation, which we attribute to the difference in the rehydration response. Three minutes of irradiation dehydrates less than at 4 min of irradiation and therefore the change in rehydration is less impactful. Five minutes of irradiation has a higher degree of dehydration on the sample, which causes increased stiffness. During rehydration of the irradiated area, the sample becomes more stretchable, and its adhesion efficiency therefore increases. In the time span of 3–5 h, the sample is still not as rehydrated as the sample which has been irradiated for 4 min. On the other hand, the interfaces undergo excessive dehydration and stiffening when the irradiation lasted for 5 min, resulting in a decrease in the adhesion strength to $56.4 \pm 23.0\%$. The stiffening can also be observed in the tensile test curve shown in Figure 3b, where the self-adhered sample after 5 min of irradiation shows a higher modulus and a smaller strain at failure. The increased ultimate tensile strength for the 5 min sample is also due to dehydration, also observed in the as-prepared hydrogel in Figure 2a. Importantly, the self-adhered hydrogels show the opposite trend in the adhesion strength compared to the self-healing hydrogels, where the self-healing efficiency increases with time until certain maximum.² In the present self-adhered hydrogels, the adhesion strength decreases with time due to rehydration of the irradiated area and gradual disentanglement of the polymer chains (Figure 3c–f). The individual measurements of the self-adhered samples can be found in Figure S7. After 3 min of irradiation, the hydrogel is able to maintain an adhesion efficiency at around $58.9 \pm 14.7\%$ for 3 h, after which the efficiency decreases to $8.9 \pm 9.3\%$ at 5 h (Figure 3d). For 4 min of irradiation, the adhesion efficiency is $95.7 \pm 25.5\%$ right after irradiation but declines to $5.9 \pm 6.9\%$ after 7 h. Curiously, the adhesion efficiency of 5 min sample (Figure 3f) reaches its maximum of $74.5 \pm 15.7\%$ at 3 h after the irradiation,

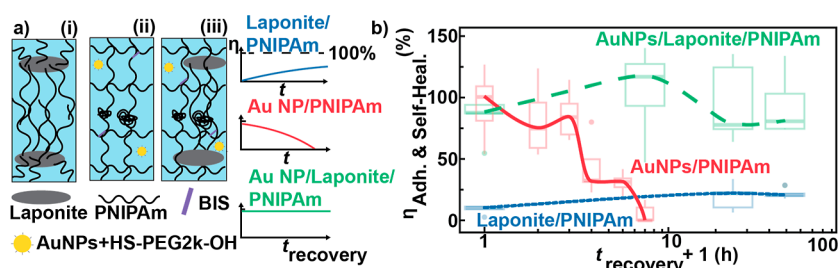


Figure 4. Synergistic combination of self-healing and self-adhesion mechanisms. (a) Illustrations of self-healing (i), self-adhesion (ii), and combined (iii) mechanisms and their typical response over time. (b) Measurement of time-dependent interfacial strength measured by recovery of strain at failure for PNIPAm samples containing Laponite (nonswollen), AuNPs (swollen), and AuNPs and Laponite (swollen). All samples were irradiated for 4 min. Curves are given as an eye guide for the boxplots. Tensile tests have been repeated at least 5 times.

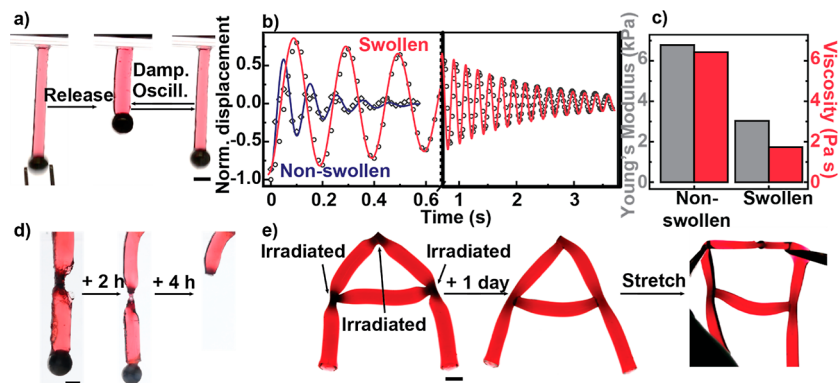


Figure 5. Demonstrations of low-hysteresis, self-adhesion, and synergistic self-healing applications. (a) Free damped oscillation of a metal sphere attached to the AuNPs/PNIPAm hydrogel. (b) Measurement of displacement during free oscillations and damping fitting. (c) Calculated Young's modulus and viscosity of nonswollen and swollen samples from the free oscillation experiment. (d) Self-adhered AuNPs/PNIPAm hydrogels with controlled release of the attached object by addition of a water droplet at 7 h. (e) Quick and permanent assembly of letter A using 3 individual AuNPs/Laponite/PNIPAm hydrogel pieces. Scale bar: 6 mm.

presumably due to the partial rehydration of collapsed polymer chains³⁶ at the interface that leads to more uniform entanglement and a higher interfacial strength. Since the interface is largely dehydrated, a longer time is needed for water to diffuse back to the interface, resulting in the more durable adhesion at the interface. In addition, increasing the polymer content of PNIPAm to 20 wt % and reducing the BIS concentration to 0.0001 mol % also resulted in a similar self-adhesion effect (Figure S8).

2.4. Synergistic Effect between Self-Adhesion and Self-Healing. Notably, the present quick self-adhesion concept can be coupled with conventional slow self-healing mechanisms to achieve a synergistic combination of both time-dependent effects. The classic self-healing mechanism provides a time-dependent increase in the interfacial strength, while the initial strength upon reattachment is typically weak, for instance in nanocomposite Laponite/PNIPAm hydrogels, which requires tens of hours to achieve 100% self-healing (Figure 4a(i)).³⁴ By contrast, the present self-adhesion mechanism allows fast realization of high initial adhesion strength within a few minutes, which then decreases with time due to the lack of dynamic bonds (Figure 4a(ii)). We next exemplify the synergistic combination of the two different mechanisms in a AuNPs/Laponite/PNIPAm hydrogel in Figure 4. Due to the chemical cross-linking of the PNIPAm network, which decreases the self-healing efficiency,⁸ the Laponite/PNIPAm hydrogel shows a minor increase in the self-healing strength to $21.5 \pm 3.4\%$ even after 48 h. However, by first inducing the self-adhesion in the AuNPs/Laponite/

PNIPAm hydrogel, an initial high adhesion efficiency of around $83.5 \pm 14.8\%$ can quickly be achieved (Figure 4b). The adhesion efficiency slowly increases with time and remains at almost $84.5 \pm 35.6\%$ up to 48 h, in strong contrast to the temporary self-adhesion in AuNPs/PNIPAm hydrogels. The results indicate that a synergistic effect took place where the initial temporary self-adhesion transitioned into self-healing between the PNIPAm and the Laponite platelet. Control experiments show that the Laponite/PNIPAm hydrogel without AuNPs do not form adhered interfaces under irradiation (Figure S9). We postulate that the light-triggered entanglement of the PNIPAm network also assisted in adsorption of the PNIPAm chains on to the Laponite platelets as the self-healing mechanism,³⁴ and thus the high interfacial strength remained throughout the tested time frame.

2.5. Application Demonstrations of Low-Hysteresis and Time-Programmable Adhesion. In Figure 5, we demonstrate the application potential of low-hysteresis and light-triggered self-adhesion in the hydrogels. Low hysteresis indicates low loss of elastic energy during deformations, which is a highly desired property, e.g., resilience and precise control of shapes in soft robots.²⁸ Figure 5a–c shows the free damped oscillation of a metal sphere attached to a piece of low-hysteresis (swollen) or high-hysteresis (nonswollen) AuNPs/PNIPAm hydrogel. The metal sphere (weight = 2 g) was attached to the free end of the hydrogel (Figure 5a), which was then elongated and released to freely oscillate. The displacement of the metal sphere was measured and is shown in Figure 5b. The swollen hydrogel clearly produced much lower

damping of the oscillation and longer oscillations for more than 4 s compared to the nonswollen hydrogel, which fully damped below 1 s. The damping in both cases can be fitted with a damped harmonic oscillator equation; see the [Supporting Information](#). The damping coefficient of nonswollen hydrogels in the fitting equation is roughly ten times higher than that of swollen hydrogels, which is in good accordance with the previously observed low hysteresis. In addition, the Young's modulus and viscosity could be calculated using the damped oscillation equations. The Young's modulus is calculated as

$$E = \frac{4\pi f^2 mL_0}{r^2} \quad (3)$$

where f represents the oscillation frequency, m is the mass of the metal sphere, and L_0 and r are the length and radius of the cylindrical sample at rest of $E = 6.78$ kPa for the nonswollen sample and 3.03 kPa for the swollen sample, respectively.

The viscosities of the samples were calculated as

$$\eta = \frac{2mL_0}{\pi t_0 r^2} \quad (4)$$

where t_0 represents the oscillation decay time. According to the analysis, η is 6.43 Pa s for the nonswollen sample and 1.73 Pa s for the swollen sample. Derivation of the equations can be found in the [Supporting Information](#). The results are summarized in [Figure S5c](#), where it can be clearly seen that both the Young's modulus and the viscosity decreased dramatically upon swelling, while the viscosity decreased more than the Young's modulus. Therefore, the ratio of Young's modulus to viscosity in the swollen sample is much higher than that in the nonswollen hydrogel, which explains the lower hysteresis due to increased elasticity.

On the other hand, the self-adhesion mechanism can be utilized for temporal control over the nonpermanent adhesion strength, which is conceptually desired, for example, in wound dressing.¹⁶ [Figure S5d](#) shows the time-controlled on-demand detachment of an adhered weight using the self-adhered hydrogels. After the irradiation treatment, a sample has been stuck to the ceiling of a box with a metal weight (2 g), and then the relative humidity of the box has been increased to 100%.

The interface initially preserved sufficient strength to withhold the weight, and the weight was spontaneously released after 6 h due to the decreased adhesive strength. Additionally, the release of the weight can also be readily triggered on demand by the addition of water to the interface, which provides additional temporal control over the interfacial strength ([Figure S10](#)).

Another key feature of the self-adhesion mechanism is that any surfaces of the hydrogel can be adhered on-demand, which does not require a freshly cut surface as in many self-healing hydrogels. We demonstrate the potential of this feature by assembling simple cylindrical hydrogels into designed shapes, as exemplified in [Figure S5e](#). Letter A was constructed by irradiation at dedicated points in three pieces of hydrogels, which formed permanently adhered and healed interfaces due to the presence of Laponite platelets. After storage for 1 day in an undeformed state at 21 °C and 99% relative humidity, see [Figure S11](#), the assembled object preserved its structural integrity and can withstand large deformations as shown in [Figures S5e](#) and [S12](#). Such property can be potentially utilized

for quick prototyping of soft objects with designed shapes, such as for soft robotic applications.

3. CONCLUSIONS

We demonstrate low hysteresis and light-triggered transient time-programmed on-demand self-adhesion in a swollen AuNPs/PNIPAm nanocomposite hydrogel. Quick and strong self-adhesion is achieved by efficient photothermal heating of AuNPs inside the PNIPAm network. Upon the phase transition induced by heating for a couple of minutes, the polymer chains at the interface strongly entangle to achieve an adhesion efficiency close to 100% measured by the tensile strain at failure. After turning the light off, the entangled chains gradually disentangle via rehydration of the interface by water diffusion from the bulk, which results in the decrease of adhesion strength to almost 0 after 7 h. The mechanical properties and recovery of strain are programmable with irradiation time. Notably, the self-adhesion mechanism can be combined with the self-healing mechanism in conventional Laponite-based nanocomposite hydrogels, which allows quick and strong self-adhesion and -healing, thus reducing the typical time of dozens of hours to a few minutes in self-healing hydrogels. We also demonstrate the application potential of the hydrogel in free damped oscillations of a metal-weight, time-programmed release of the adhered weight, and quick and permanent assembly of simple hydrogel shapes into designed geometries. The reported self-adhesion mechanism and demonstrations provide implications for self-healing and self-adhesive soft materials and their application potential in soft robotics or biomedical applications.

4. METHODS

4.1. Materials. *N*-Isopropylacrylamide (NIPAm, ≥99%), *N,N,N',N'*-tetramethylethylenediamine (TEMED, 99%), potassium persulfate (KPS, ≥99.0%), sodium citrate tribasic dihydrate (≥99.5%), gold(III) chloride trihydrate (≥99.9%), acrylamide (≥99%), APS (≥98%), and poly(ethylene glycol)methyl ether thiol (OH-PEG2k-SH, $M_w = 2000$) were purchased from Sigma-Aldrich. Deionized water (Milli-Q) was used throughout the experiments.

4.2. Gold Nanoparticle Synthesis. 37.91 mg of gold chloride trihydrate was dissolved in 100 mL of water with 205.99 μL of sodium hydroxide (1.0 M). The solution was brought to the boiling point in an oil bath, and 880 μL of citrate tribasic dihydrate (100 mg mL⁻¹) was quickly injected into the solution under vigorous stirring. After 20 min of continuous refluxing, the solution containing AuNPs was taken out of the bath. After cooling, 3 mg of OH-PEG2k-SH was added to 80 mL of AuNPs solution, which was incubated overnight. The solution was purified three times by centrifugation at 10,000g for 30 min, removal of the supernatant, and redilution to the original volume. Finally, a concentrated stock solution of 2 mL was obtained, which contained 4 mg mL⁻¹ AuNPs.

4.3. Hydrogel Synthesis. 160 mg of NIPAm was dissolved in 735 μL of water, to which 10 μL of BIS solution (10 mg mL⁻¹) and 250 μL of AuNPs solution (4 mg mL⁻¹) were added. The solution was vortexed and then bubbled with nitrogen for 5 min to remove the oxygen. Afterward, 5 μL of APS aqueous solution (10 wt %) and 0.5 μL of TEMED were added and gently stirred. The solution was quickly injected into glass tubes in nitrogen-purged vials at 20 °C for polymerization. After 2 h, the samples were taken out of the tubes and put into Milli-Q water overnight.

4.4. Tensile Testing. The Instron model 5567 tensile tester with a 100 N load cell was used. The traverse speed was 100% min⁻¹.

4.5. Resilience Testing. For resilience testing, samples were allowed to soak overnight in a Milli-Q water-filled vial. The traverse speed was 100% min⁻¹. Fatigue resistance was tested by repeating the cyclic tensile test for several cycles in a 100% relative humidity

environment. The area below the curve was determined by integrating via the trapezoidal rule between each measurement step.

4.6. Light-Induced Self-Adhesion Tests. Either a cut sample or two different samples were used for light-induced self-adhesion testing. The surfaces of the connecting site were adhered to each other and then irradiated by a LED (Thorlabs Solis-S25C) at a power of 2.4 W. The room humidity was controlled to be 30% RH during irradiation. Then, the samples were transferred to the tensile tester after storage in a closed vessel with 5 water droplets for certain durations. The traverse speed was 100% min⁻¹.

4.7. Step Strain Testing. A sample was extended until a strain of 2 at a traverse speed of 200% s⁻¹, and then it was held at the same strain for 5 min.

4.8. Free Damped Oscillation. A metal ball (weight = 2 g) was adhered to one end of a hydrogel sample with a length of 20 mm. The hydrogel sample was stretched by 10 mm, and the ball was released to freely oscillate. Videos were captured with a Canon 80D camera, and the position of the metal ball was analyzed by the tracking software Kinovea (V0.9.5).

4.9. Numerical Simulation. The simulation of the photothermal heating process was carried out in COMSOL Multiphysics 5.5. A cylindrical piece of hydrogel was fabricated on top of a Teflon substrate with the same dimensions as used in the experiments. The hydrogel was assumed to have the same physical properties as water, and the physical properties from COMSOL's library were directly used. The heat transfer in the solid module was coupled with the radiative beam in the absorbing media module to reflect the photothermal heating process of a Gaussian beam with a power of 2.3 W. A time-dependent study was used with a step size of 1 s.

■ ASSOCIATED CONTENT

SI Supporting Information

The Supporting Information is available free of charge at <https://pubs.acs.org/doi/10.1021/acsapm.3c02117>.

Additional experimental details, materials and methods, additional parameters of simulation, additional photographs of samples, and additional characterization details of materials (PDF)

■ AUTHOR INFORMATION

Corresponding Authors

Olli Ikkala – Department of Applied Physics, Aalto University, FI 02150 Espoo, Finland; orcid.org/0000-0002-0470-1889; Email: olli.ikkala@aalto.fi

Hang Zhang – Department of Applied Physics, Aalto University, FI 02150 Espoo, Finland; orcid.org/0000-0003-4949-3371; Email: hang.zhang@aalto.fi

Authors

Henri Savolainen – Department of Applied Physics, Aalto University, FI 02150 Espoo, Finland

Matilda Backholm – Department of Applied Physics, Aalto University, FI 02150 Espoo, Finland

Complete contact information is available at: <https://pubs.acs.org/doi/10.1021/acsapm.3c02117>

Author Contributions

H.Z. conceptualized the project. H.S. performed the experiments. H.S., O.I., M.B., and H.Z. analyzed the data. M.B. performed the calculation of viscosity and modulus. H.Z. performed numerical simulations. All authors contributed to the writing of the manuscript. All authors have given approval to the final version of the manuscript.

Funding

Funding was received from the Academy of Finland.

Notes

The authors declare no competing financial interest.

■ ACKNOWLEDGMENTS

We thank Dr. Zhongpeng Lyu for his help with the low hysteresis measurement and Amanda Eklund for help with the transmittance measurement. We thank the Aalto University at OtaNano—Nanoscience Center (Aalto-NMC) for provision of facilities and technical support. We acknowledge funding from the Academy of Finland (Postdoctoral Researcher no. 331015 to H.Z., Postdoctoral Researcher no. 309237 to M.B., and Project SPIKING no. 334433 to O.I.).

■ REFERENCES

- (1) Ge, G.; Lu, Y.; Qu, X.; Zhao, W.; Ren, Y.; Wang, W.; Wang, Q.; Huang, W.; Dong, X. Muscle-Inspired Self-Healing Hydrogels for Strain and Temperature Sensor. *ACS Nano* **2020**, *14* (1), 218–228.
- (2) Taylor, D. L.; in het Panhuis, M. Self-Healing Hydrogels. *Adv. Mater.* **2016**, *28* (41), 9060–9093.
- (3) Qin, H.; Liu, P.; Chen, C.; Cong, H.-P.; Yu, S.-H. A Multi-Responsive Healable Supercapacitor. *Nat. Commun.* **2021**, *12* (1), 4297.
- (4) Qin, H.; Zhang, T.; Li, N.; Cong, H.-P.; Yu, S.-H. Anisotropic and Self-Healing Hydrogels with Multi-Responsive Actuating Capability. *Nat. Commun.* **2019**, *10* (1), 2202.
- (5) Qin, H.; Zhang, T.; Li, H.-N.; Cong, H.-P.; Antonietti, M.; Yu, S.-H. Dynamic Au-Thiolate Interaction Induced Rapid Self-Healing Nanocomposite Hydrogels with Remarkable Mechanical Behaviors. *Chem* **2017**, *3* (4), 691–705.
- (6) Perera, M. M.; Ayres, N. Dynamic Covalent Bonds in Self-Healing, Shape Memory, and Controllable Stiffness Hydrogels. *Polym. Chem.* **2020**, *11* (8), 1410–1423.
- (7) Zhang, H.; Xia, H.; Zhao, Y. Poly(Vinyl Alcohol) Hydrogel Can Autonomously Self-Heal. *ACS Macro Lett.* **2012**, *1* (11), 1233–1236.
- (8) Ihsan, A. B.; Sun, T. L.; Kurokawa, T.; Karobi, S. N.; Nakajima, T.; Nonoyama, T.; Roy, C. K.; Luo, F.; Gong, J. P. Self-Healing Behaviors of Tough Polyampholyte Hydrogels. *Macromolecules* **2016**, *49* (11), 4245–4252.
- (9) Tuncaboylu, D. C.; Sari, M.; Oppermann, W.; Okay, O. Tough and Self-Healing Hydrogels Formed via Hydrophobic Interactions. *Macromolecules* **2011**, *44* (12), 4997–5005.
- (10) Nakahata, M.; Takashima, Y.; Harada, A. Highly Flexible, Tough, and Self-Healing Supramolecular Polymeric Materials Using Host-Guest Interaction. *Macromol. Rapid Commun.* **2016**, *37* (1), 86–92.
- (11) Luo, F.; Sun, T. L.; Nakajima, T.; Kurokawa, T.; Zhao, Y.; Sato, K.; Ihsan, A. B.; Li, X.; Guo, H.; Gong, J. P. Oppositely Charged Polyelectrolytes Form Tough, Self-Healing, and Rebuildable Hydrogels. *Adv. Mater.* **2015**, *27* (17), 2722–2727.
- (12) Nian, G.; Kim, J.; Bao, X.; Suo, Z. Making Highly Elastic and Tough Hydrogels from Doughs. *Adv. Mater.* **2022**, *34*, 2206577.
- (13) Su, X.; Mahalingam, S.; Edirisinghe, M.; Chen, B. Highly Stretchable and Highly Resilient Polymer-Clay Nanocomposite Hydrogels with Low Hysteresis. *ACS Appl. Mater. Interfaces* **2017**, *9* (27), 22223–22234.
- (14) Wang, Y.; Yu, X.; Zhang, H.; Fan, X.; Zhang, Y.; Li, Z.; Miao, Y.-E.; Zhang, X.; Liu, T. Highly Stretchable, Soft, Low-Hysteresis, and Self-Healable Ionic Conductive Elastomers Enabled by Long, Functional Cross-Linkers. *Macromolecules* **2022**, *55* (17), 7845–7855.
- (15) Kong, W.; Yang, Y.; Wang, Y.; Cheng, H.; Yan, P.; Huang, L.; Ning, J.; Zeng, F.; Cai, X.; Wang, M. An Ultra-Low Hysteresis, Self-Healing and Stretchable Conductor Based on Dynamic Disulfide Covalent Adaptable Networks. *J. Mater. Chem. A* **2022**, *10* (4), 2012–2020.
- (16) Yang, J.; Bai, R.; Chen, B.; Suo, Z. Hydrogel Adhesion: A Supramolecular Synergy of Chemistry, Topology, and Mechanics. *Adv. Funct. Mater.* **2020**, *30* (2), 1901693.

- (17) Guo, Z.; Mi, S.; Sun, W. The Multifaceted Nature of Catechol Chemistry: Bioinspired PH-Initiated Hyaluronic Acid Hydrogels with Tunable Cohesive and Adhesive Properties. *J. Mater. Chem. B* **2018**, *6* (39), 6234–6244.
- (18) Liu, Y.; Wang, P.; Su, X.; Xu, L.; Tian, Z.; Wang, H.; Ji, G.; Huang, J. Electrically Programmable Interfacial Adhesion for Ultrastrong Hydrogel Bonding. *Adv. Mater.* **2022**, *34* (13), 2108820.
- (19) Eklund, A.; Ikkala, O.; Zhang, H. Highly Efficient Switchable Underwater Adhesion in Channeled Hydrogel Networks. *Adv. Funct. Mater.* **2023**, 2214091.
- (20) Gao, Y.; Wu, K.; Suo, Z. Photodetachable Adhesion. *Adv. Mater.* **2019**, *31* (6), 1806948.
- (21) Yi, Y.; Xie, C.; Liu, J.; Zheng, Y.; Wang, J.; Lu, X. Self-Adhesive Hydrogels for Tissue Engineering. *J. Mater. Chem. B* **2021**, *9* (42), 8739–8767.
- (22) Deng, X.; Attalla, R.; Sadowski, L. P.; Chen, M.; Majcher, M. J.; Urosev, I.; Yin, D.-C.; Selvaganapathy, P. R.; Filipe, C. D. M.; Hoare, T. Autonomously Self-Adhesive Hydrogels as Building Blocks for Additive Manufacturing. *Biomacromolecules* **2018**, *19* (1), 62–70.
- (23) Xie, C.; Wang, X.; He, H.; Ding, Y.; Lu, X. Mussel-Inspired Hydrogels for Self-Adhesive Bioelectronics. *Adv. Funct. Mater.* **2020**, *30* (25), 1909954.
- (24) Mourran, A.; Zhang, H.; Vinokur, R.; Möller, M. Soft Microrobots Employing Nonequilibrium Actuation via Plasmonic Heating. *Adv. Mater.* **2017**, *29* (2), 1604825.
- (25) Shiotani, A.; Mori, T.; Niidome, T.; Niidome, Y.; Katayama, Y. Stable Incorporation of Gold Nanorods into N-Isopropylacrylamide Hydrogels and Their Rapid Shrinkage Induced by Near-Infrared Laser Irradiation. *Langmuir* **2007**, *23* (7), 4012–4018.
- (26) Qin, H.; Zhang, T.; Li, H.-N.; Cong, H.-P.; Antonietti, M.; Yu, S.-H. Dynamic Au-Thiolate Interaction Induced Rapid Self-Healing Nanocomposite Hydrogels with Remarkable Mechanical Behaviors. *Chem* **2017**, *3* (4), 691–705.
- (27) Pelton, R. Poly(N-Isopropylacrylamide) (PNIPAM) Is Never Hydrophobic. *J. Colloid Interface Sci.* **2010**, *348* (2), 673–674.
- (28) Yang, Q.; Shamsavan, H.; Deng, Z.; Guo, H.; Zhang, H.; Liu, H.; Zhang, C.; Priimagi, A.; Zhang, X.; Zeng, H. Semi-Crystalline Rubber as a Light-Responsive, Programmable, Resilient Robotic Material. *Adv. Funct. Mater.* **2022**, *32* (41), 2206939.
- (29) Liu, C.; Morimoto, N.; Jiang, L.; Kawahara, S.; Noritomi, T.; Yokoyama, H.; Mayumi, K.; Ito, K. Tough Hydrogels with Rapid Self-Reinforcement. *Science* **2021**, *372* (6546), 1078–1081.
- (30) Meng, X.; Qiao, Y.; Do, C.; Bras, W.; He, C.; Ke, Y.; Russell, T. P.; Qiu, D. Hysteresis-Free Nanoparticle-Reinforced Hydrogels. *Adv. Mater.* **2022**, *34* (7), 2108243.
- (31) Baumgartner, M.; Hartmann, F.; Drack, M.; Preninger, D.; Wirthl, D.; Gerstmayr, R.; Lehner, L.; Mao, G.; Pruckner, R.; Demchyshyn, S.; Reiter, L.; Strobel, M.; Stockinger, T.; Schiller, D.; Kimeswenger, S.; Greibich, F.; Buchberger, G.; Bradt, E.; Hild, S.; Bauer, S.; Kaltenbrunner, M. Resilient yet Entirely Degradable Gelatin-Based Biogels for Soft Robots and Electronics. *Nat. Mater.* **2020**, *19* (10), 1102–1109.
- (32) Yamamoto, T.; Campbell, J. A.; Panyukov, S.; Rubinstein, M. Scaling Theory of Swelling and Deswelling of Polymer Networks. *Macromolecules* **2022**, *55* (9), 3588–3601.
- (33) Kim, J.; Zhang, G.; Shi, M.; Suo, Z. Fracture, Fatigue, and Friction of Polymers in Which Entanglements Greatly Outnumber Cross-Links. *Science* **2021**, *374* (6564), 212–216.
- (34) Haraguchi, K.; Uyama, K.; Tanimoto, H. Self-Healing in Nanocomposite Hydrogels. *Macromol. Rapid Commun.* **2011**, *32* (16), 1253–1258.
- (35) Wang, Y.; Nian, G.; Kim, J.; Suo, Z. Polyacrylamide Hydrogels. VI. Synthesis-Property Relation. *J. Mech. Phys. Solids* **2023**, *170*, 105099.
- (36) Sun, S.; Hu, J.; Tang, H.; Wu, P. Chain Collapse and Revival Thermodynamics of Poly(N-Isopropylacrylamide) Hydrogel. *J. Phys. Chem. B* **2010**, *114* (30), 9761–9770.